Scanning Microscopy Vol. 12, No. 3, 1998 (Pages 437-448) 0891-7035/98$5.00+.25
Scanning Microscopy International, Chicago (AMF O'Hare), IL 60666 USA

# FORMATION AND INTERACTION OF HOLLOW NEON ATOMS AT AN ALUMINUM SURFACE

N. Stolterfoht[1]*, D. Niemann[1], M. Grether[1], A. Spieler[1] and A. Arnau[2]

[1]Hahn-Meitner Institut, Bereich Festkörperphysik, Glienickerstr. 100, D-10109 Berlin, Germany
[2]Departamento de Física de Materiales, Universidad de País Vasco, San Sebastían, Spain

(Received for publication May 13, 1996 and in revised form February 11, 1997)

**Abstract**

Theoretical and experimental methods were used to study the interaction of $Ne^{9+}$ ions with an Al surface. Theoretical models were applied to visualize the shape and dimension of hollow neon atoms formed above and below the surface. Atomic Hartree-Fock calculations were performed to determine the large hollow atoms produced with electrons in high Rydberg levels above the surface. Inside the first surface layers hollow atoms were evaluated by means of a Density Functional theory including non-linear screening effects. The time-dependent decay sequence of a hollow atom was determined from a cascade model that describes the filling of the L shell. The cascade model yields information about the life time and the interaction region of the hollow atom within the first layers of the surface. Experimental results obtained by means of Auger spectroscopy are used to verify the results of the model predictions.

**Key Words**: Multiply charged ions, low velocities, hollow atoms, self consistent field calculations, dynamic screening, electron spectroscopy, ultra-high vacuum, K Auger spectra.

*Address for correspondence:
N. Stolterfoht
Hahn-Meitner Institut, Bereich Festkörperphysik
Glienickerstr. 100
D-10109 Berlin, Germany
Telephone number: (30) 8062-2340
FAX number: (30) 8062-2293
E-mail: Stolterfoht@hmi.de

## Introduction

Studies of slow, highly charged ions interacting with surfaces have received considerable attention in the past few years [1-9, 12, 15, 20, 22]. When a slow and highly charged ion approaches a surface, several electrons are resonantly transferred from the conduction band of the solid to the ion. Figure 1 gives an overview over the associated mechanisms. In front of the surface, a "hollow" atom is produced by charge transfer with many electrons in higher Rydberg orbitals and empty intermediate shells [7, 8]. Auger transitions in the Rydberg orbitals results in a shrinking of the charge cloud around the ion [2]. Also, as the ion approaches the surface, the electrons in higher Rydberg orbitals are removed and lower lying orbitals become occupied. When the ion enters into the surface, a final peel-off of the Rydberg electrons occurs so that a highly charged ion is again produced [5, 8]. The highly charged ion strongly attracts electrons from the solid and, hence, it produces an electron cloud dynamically screening the nuclear charge [3, 11].

Inside the solid, the electron cloud induced by slow ions has essentially a spherical shape. The production of this cloud, labeled C in the inset of Figure 1, is the outstanding property of a slow, highly charged ion moving below the surface. The C cloud gives rise to a hollow whose dimension is much smaller than that outside the solid. As the hollow atom travels in the solid, the inner shell orbitals are successively filled by Auger transitions and collisional charge transfer [27].

In this work, electronic density functions are determined to visualize the electron clouds formed around the highly charged ions above and below the surface. In both cases, the induced electron densities are relatively intense so that non-linear theories are required to describe their formation. The related calculations are performed in a self-consistent manner within the frame-work of an atomic Hartree-Fock method and a density-functional approach. The calculations yield wave functions for the associated orbitals that can be used to obtain a realistic picture of the electron density formed around the highly charged ion. Moreover, the calculation provides Auger transition energies that can be compared with experiment.

The experiments were carried out at an electron-

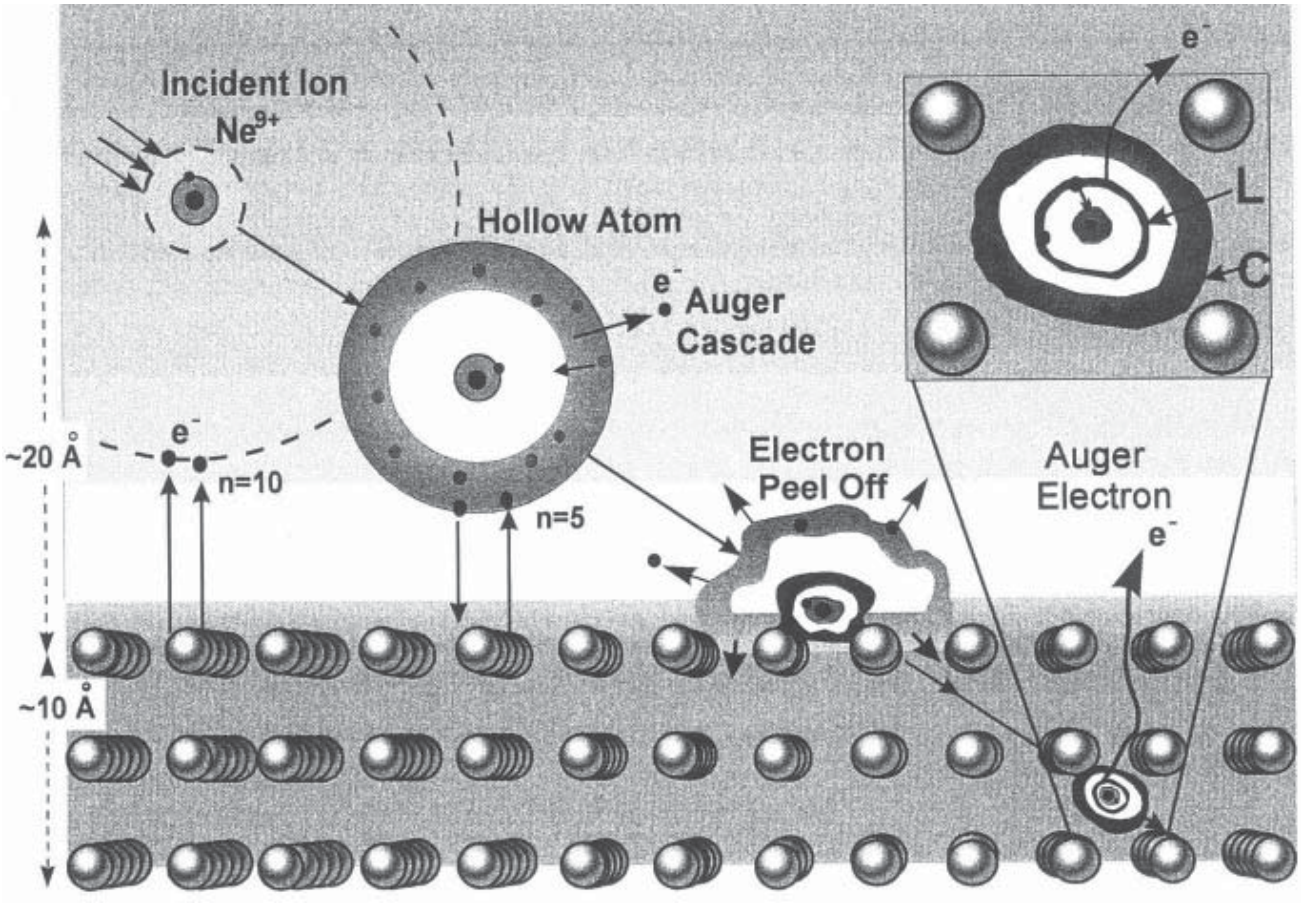


**Figure 1**. Formation of hollow atoms above and below the surface. In the solid the ion with an empty L shell induces the electron cloud, labeled C.

cyclotron resonance (ECR) source that included a deceleration system, which allowed for the production of very slow ions at energies as low as a few tens of eV. In this contribution, we report on experimental work performed with $Ne^{9+}$ incident on an Al target. The data was taken using Auger spectroscopy. The measured Auger spectra reveal pronounced structures that can be attributed to the filling state of the hollow atom.

Hence, Auger spectroscopy is well suited to gain information about dynamic properties of a hollow atom moving just below the surface. The relatively fast Auger transitions serve as a unique "clock" to measure the time dependent phenomena within the $10^{-15}$ second time scale. Besides the Auger transitions, collisional vacancy transfer from target atoms contributes to the filling mechanisms. We present a cascade model for the filling sequence of empty orbitals providing information about the life time and the interaction region of the hollow atom within the first layers of the surface.

## Experimental Methods

The experiments were performed using the 14.5-GHz ECR source at the Ionenstrahl-Labor (ISL) of the Hahn-Meitner-Institut in Berlin [19]. The ion source provides projectiles with energies up to 20q keV, where q is the charge state of the extracted ions. The end of the beam line is equipped with a deceleration lens system to extract ions at energies as low as 5q eV. The beam line can be set on a high-voltage potential so that the experimental apparatus can be operated on ground potential.

For the experiments, an ultra-high-vacuum chamber designed for electron spectroscopy was used. The apparatus has been described in detail previously [15]. The base pressure during the measurements was a few $10^{-10}$ mbar. The vacuum chamber includes facilities for surface preparation and examination. Auger electron spectroscopy was used to verify the cleanness of the surface. After careful cleaning, no

contaminations of the surface by C, N, and O could be observed.

Highly charged, hydrogen-like $Ne^{9+}$ was used to bombard an Al target. After the ions were accelerated, they were magnetically analyzed and collimated to a diameter of about 1 mm at the position of the target. The beam diameter was determined by measuring the ion current on a thin wire by scanning the wire through the beam at the target position. Electrons ejected by the interaction of the ions with the surface were measured with an electrostatic parallel-plate spectrometer whose observation angle could be varied widely. The electron spectra were normalized to an absolute scale, taking into account the acceptance angle, resolution, and spectrometer transmission and the efficiency of the channeltron. For more details concerning the normalization of the Auger spectra, see the work by Köhrbrück *et al.* [15].

Typical examples of the Auger electron spectra are given in Figure 2. To demonstrate the influence of the solid, the spectrum obtained with a solid Al target is compared with previous results using a He gas target [14]. In the latter case, the projectile with an initial configuration $1s^22s^2$ is ionized in the 1s shell so that the $1s^2s^{2\,2}S$ state is produced. It decays via $KL_1L_1$ Auger transitions into the final state $1s^{2\,1}S$, giving rise to mono-energetic electrons with an energy of 652 eV. Another Auger maximum, observed at higher energies, is due to the configuration $1s2s2p$ produced by $1s$ ionization of the projectiles in the initial metastable state $1s^22s2p^3P_0$ [14].

The spectrum obtained with $Ne^{9+}$ incident on the Al target contain lines for the same $KL_1L_1$ Auger transition $1s2s^2\ {}^2S \rightarrow 1s^{2\,2}S$, but shifted by an energy as large as 95 eV. This shift is due to the influence of the solid producing screening effects, as discussed in more detail in the next sections. Here it is important to remember that the solid produces a significant energy shift. It shows that the Auger transitions can be used as sensitive probes to verify solid state properties.

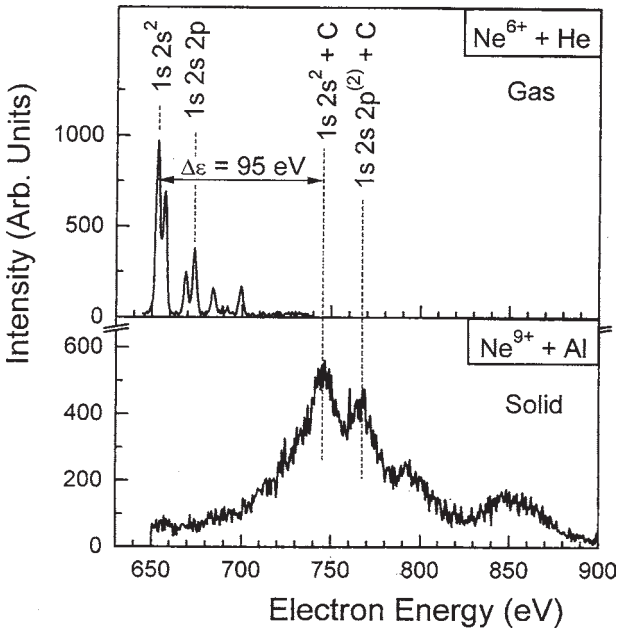


**Figure 2**. Comparison of electron spectra measured for $Ne^{q+}$ impact on He gas targets and solid Al target. The spectrum from the He target [14] exhibits a prominent Auger line at 652 eV which originates from the Auger transition $1s2s^{2\,2}S \rightarrow 1s^{2\,2}S$. The correspond-ing line is shifted by 95 eV for the Al target due to solid state effects.

## Above Surface Phenomena

The interaction of highly charged ions in front of the surface has been discussed in detail by Burgdörfer *et al.* [9] and Aumayr *et al.* [5]. When the ion approaches the surface, it is known from the classical over-barrier model that resonant charge transfer takes place into orbitals whose outer boundary just touches the surface. Hence, for different distances of the ion from the surface, Figure 3 shows orbitals whose outer radii coincide with these distances. The present picture implies that lower lying orbitals are continuously filled, while higher lying orbitals are depopulated as the ion approaches the surface. Electrons in higher lying orbitals are removed by ejection into the vacuum and, more likely, by reentering into the solid.

As noted, electrons are transferred from the conduction band into the orbitals whose outer boundary just reaches the surface. In accordance with the framework of the over-barrier model, it is assumed that the transfer of the electrons is relatively fast and that the ion is nearly neutralized [8]. Furthermore, the orbitals are assumed to be spherically symmetric, although they are likely polarized [6]. It should be realized that the present picture is over-simplified. The assumptions made here are due to idealizations in an adiabatic picture that requires ions moving at asymptotically small velocities. In spite of the simplifications, it will be shown that the present picture provides useful information that supports the basic understanding of multiply charged ion-surface interaction.

The wave functions underlying the density plots are obtained from Hartree-Fock calculations using the atomic structure code by Cowan [10]. The calculations were carried out for ions in the configuration $1s2s^2nl^7$ with core electrons in the $1s$ and $2s$ orbitals and a number of 7 Rydberg electrons in outer orbitals with the prin-cipal quantum number $n$. The orbital angular momenta $l$ stands for the lowest values 0 and 1. It should be noted that the experiment involves $Ne^{9+}$ projectiles whose 2s state is empty. The 2s occupation, and hence, the production of the configurations $1s2s^2nl^7$, are hypothetical for large $n$. Also, it is a simplifying assumption

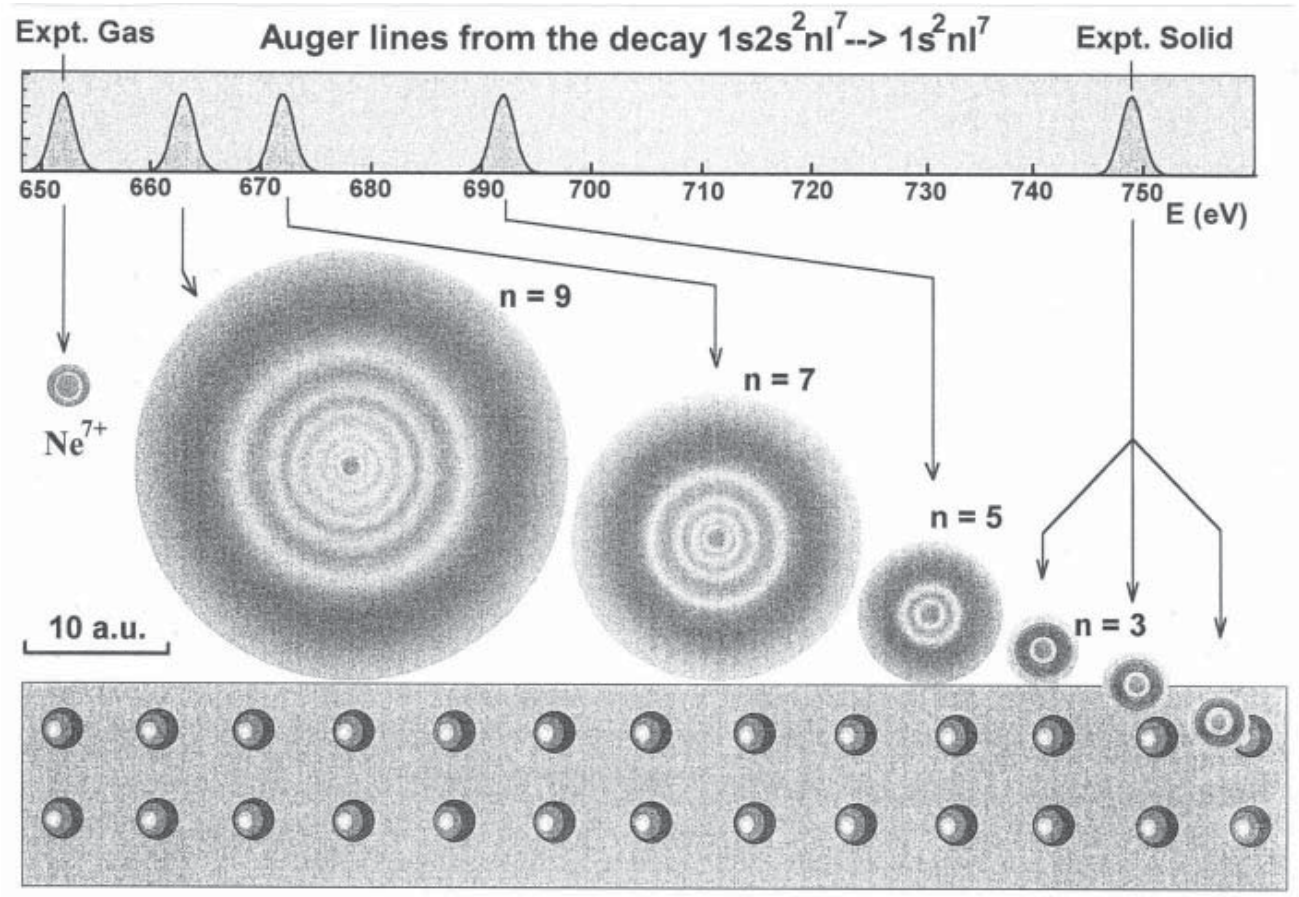


**Figure 3**. Density plot of Rydberg electrons with the principle quantum number $n = 9$, 7, 5, and 3 and $l = 1$. The plots are based on orbitals obtained from Hartree-Fock (HF) calcula-tions [10] of the configuration $1s2s^2nl^7$ where the lowest angular momenta $l = 0$ and 1 are occupied. Note the length of 10 a.u. indicated in the figure. Auger line positions, also obtained from the HF calculations, are shown on the top of the graph.

that the 7 electrons are concentrated in orbitals with a single quantum number $n$. This supposition is made to obtain information about the $n$ values present during the $KL_1L_1$ Auger transition, by comparison with experimental Auger spectra.

The Hartree-Fock calculations were conducted for the Rydberg orbitals with $n = 9$, 7, 5, and 3. Density plots of these Rydberg orbitals with angular momentum $l = 1$ are shown in Figure 3. We do not consider the population of the $n = 2$ orbitals, as the electron transfer from the conduction band is expected to be small in that case. As described further below, the $n = 2$ orbital is populated via (less probable) binary collisions near the surface. Due to the fact that the radius of the Rydberg orbitals scales with $n^2$, the orbital increases strongly in size as the quantum number $n$ increases. We note that the radius of the $n = 9$ orbital is as large as ~20 a.u. (see the length scale in the figure). On the other hand, the n = 3 orbital has a relative small radius of about ~2 a.u., i.e., its diameter is of the same order or smaller than the distance between the lattice atoms in the solid. Hence, it is expected that the dimension of the ion does not change much when entering into the solid.

The electrons in the outer Rydberg orbital influence the Auger transition energy by screening effects. This can be seen in the upper part of Figure 3, which shows the energy of the Auger lines due to the transitions $1s2s^2nl^7 \rightarrow 1s^2nl^7$, where the quantum number $n$ was varied in accordance with the density plots of the orbitals. The calculated energy of the Auger line for the atomic case $n = \infty$ is found to be in good agreement with the experiment using a gas target (Fig. 2). It is seen that the Auger line is shifted to higher energies as the radius of the occupied orbital decreases with decreasing ion-surface distance.

The important result of the Auger energy calculations is that the energy shift is relatively small for high $n$ values.

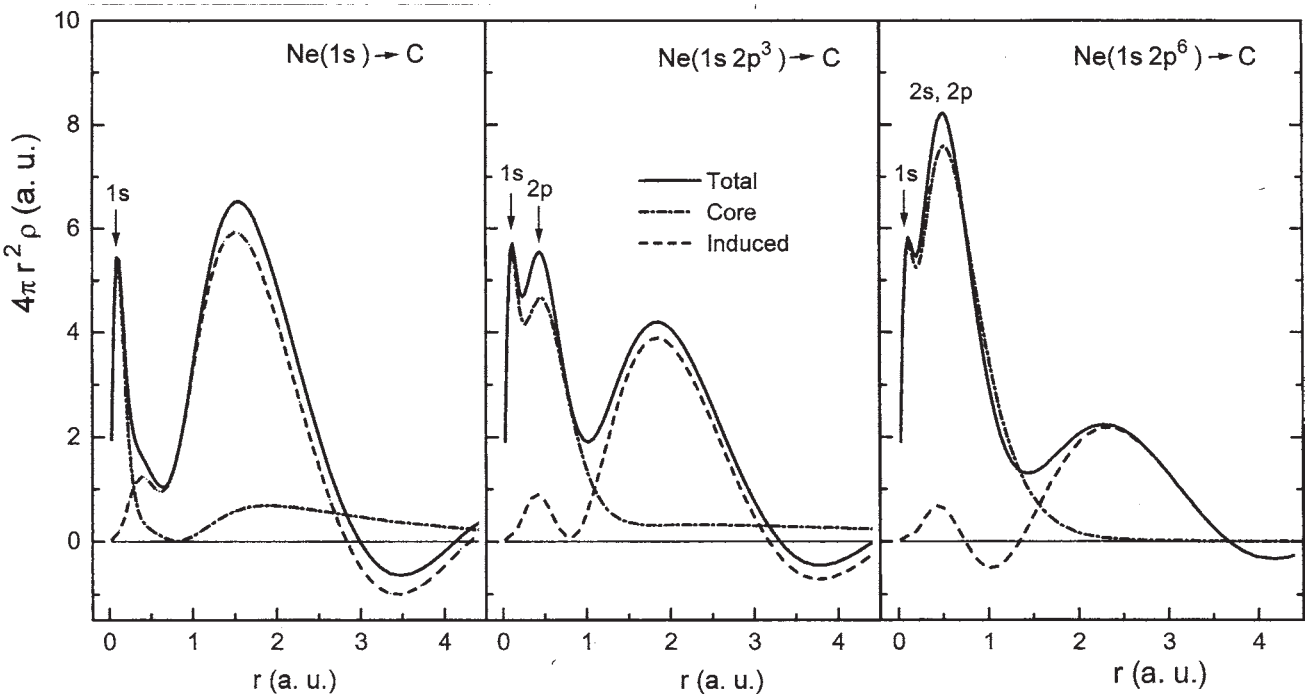


**Figure 4**. Electron densities of hollow atoms in a carbon solid calculated using the Density functional theory [28]. In the graph from the left to the right, the hollow atom has an increasing number $n_L$ = 0, 3, and 6 of L-shell electrons. The density of bound electrons (dashed-dotted curve) is given separately from the induced charge density (dotted curve). The total density (solid line) is obtained as the sum of the individual curves.

Significant energy shifts do not occur before the small values $n$ = 5 to 3 are attained. Finally, the experimental value of 748 eV (Fig. 2) for solid targets is reached for the smallest value $n$ = 3 considered here. In fact, from the dimension of the $n$ = 3 orbital, it may be concluded that the ion has a maximum distance of about 2 a.u. from the surface, i.e., the jellium edge, when the $KL_1L_1$ Auger electrons of 748 eV are ejected. This is a clear indication that the Auger electrons, observed in the experiments, originate from ions that have at least reached the surface if not entered into the solid.

Hence, the estimated distance of 2 a.u. corresponds to an upper limit for the emission of the $KL_1L_1$ Auger electrons of 748 eV. The $KL_1L_1$ Auger transitions require at least 2 electrons in the L shell. As the experiment starts with an empty 2s orbital, it takes additional time until 2 electrons are transferred into the $n$ = 2 orbital. Hence, it is probable that the ion has entered into the surface when the observed $KL_1L_1$ Auger transitions take place. The situation changes when projectiles are used under grazing incidence so that the ions are reflected from the surface [20]. However, in this work, experimental conditions are chosen where the incident ions enter into the solid.

The interaction of the ion in the solid will be discussed in the next section. However, it should already be noted that the electron cloud induced in the solid is similar to that for the $n$ = 3 orbital. Hence, the observed energy of the $KL_1L_1$ Auger electrons is consistent with the Auger emission in the 3 cases indicated in Figure 3, i.e., just above, at, or just below the surface. Additional information is required to determine the most probable location of the ion during the Auger transitions.

Such information has been achieved by Köhrbrück *et al.* [16], who studied the angular distribution of the Auger electrons. The above-surface emission of Auger electrons is expected to be isotropic, whereas below the surface, the angular distribution is anisotropic due to attenuation effects on the electrons traveling in the bulk. For the present cases, strong anisotropies were found showing that the K-Auger electrons are ejected after the ion has entered into the surface [16]. This finding is even true for the lowest projectile energy used in the experiments, in accordance with the over-the-barrier model by Burgdörfer *et al.* [9]; also see the discussion by Stolterfoht *et al.* [27].

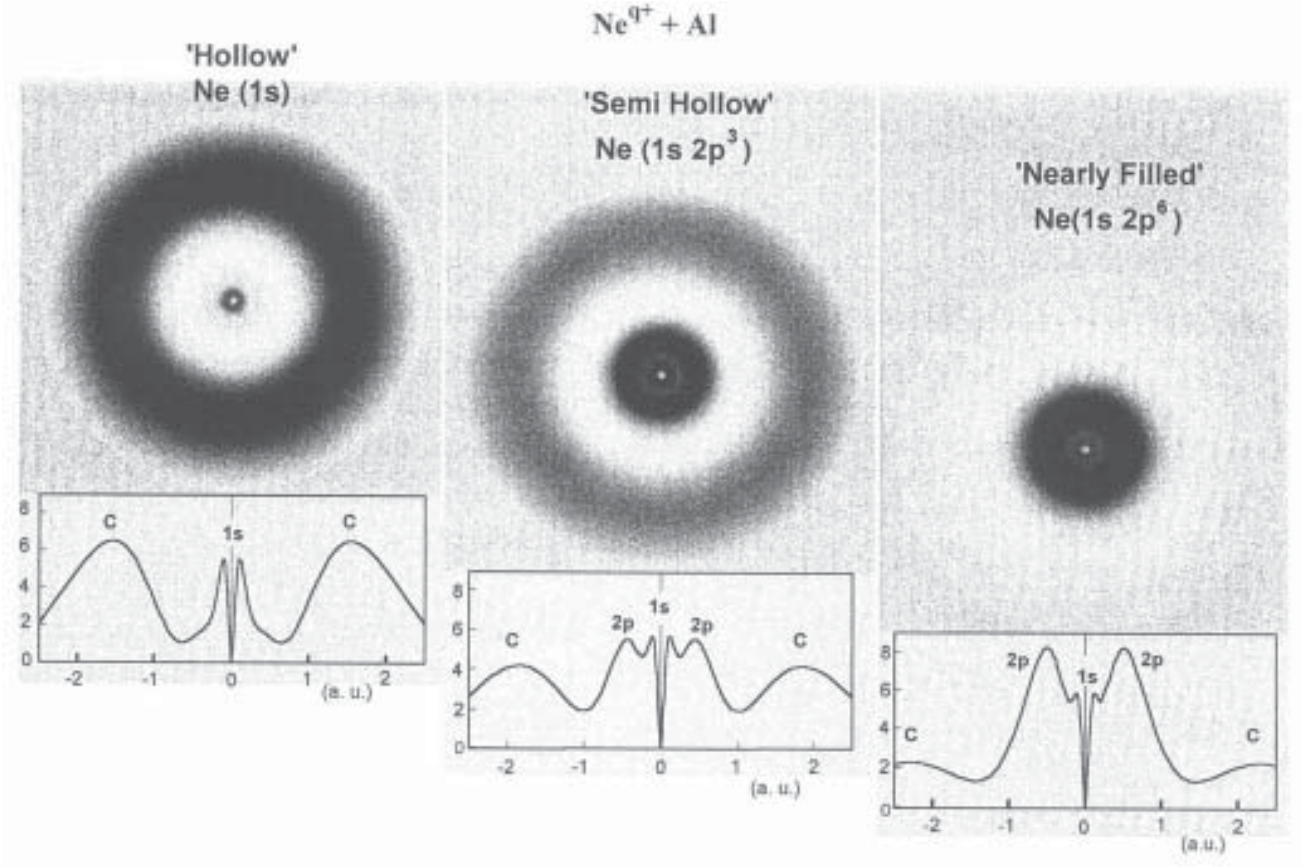


**Figure 5**. Density plots of hollow, semi-hollow, and nearly filled Ne atoms in Al. The data are calculated by means of the density functional theory [28]. The configurations of the hollow atom correspond to those used in Figure 4. Note that the density is multiplied by the square of the distance *r*.

### Below Surface Phenomena

In contrast to extensive studies of hollow atoms moving in front of the surface, less information is available about their behavior below the surface. Highly charged ions have the outstanding property that they accumulate a significant amount of charge in the solid to screen their nuclear charge. Hence, they induce the relatively large screening cloud labeled C in Figure 1. In this case, it is evident that non-linear theories are required to adequately model the C cloud in the solid.

Such a study of hollow atoms in a solid has recently been performed by Arnau *et al.* [3] who evaluated the screening function for $Ne^{9+}$ in Al using self-consistent field methods. In the analysis, the density functional theory (DFT) was applied to the problem of a static charge impurity in jellium [28]. Thus, screening functions were determined modeling the features of hollow projectile atoms. The solid-state effects are found to significantly influence the total energies of ions located as charge impurity in jellium. From total energy differences, the orbital energies for the multicharged Ne ion (with one K-shell vacancy) in Al were calculated. More details are given in the work by Arnau *et al*. [3].

Examples of the DFT calculations are shown in Figure 4 referring to hollow Ne atoms in C. In the graphs from the left to the right, the atom has an increasing number $n_L$ of electrons in the L shell. The electrons bound in the K and L shell (dashed-dotted line) are shown separately from the induced charge cloud (dashed line). The calculations indicate that at its maximum, the induced charge cloud is about a factor of 5 higher in density as the jellium background (not shown in the figure). This clearly confirms the remarkable property of the hollow atom formed by a highly charged ion, i.e., the large charge cloud induced within the solid.

As expected, the induced charge cloud decreases in intensity as the filling state $n_L$ of the L shell increases. As the hollow atom is neutral, the number of electrons contained in the induced charge cloud is equal to the number of electrons missing in the core. For instance, a hollow atom with one K

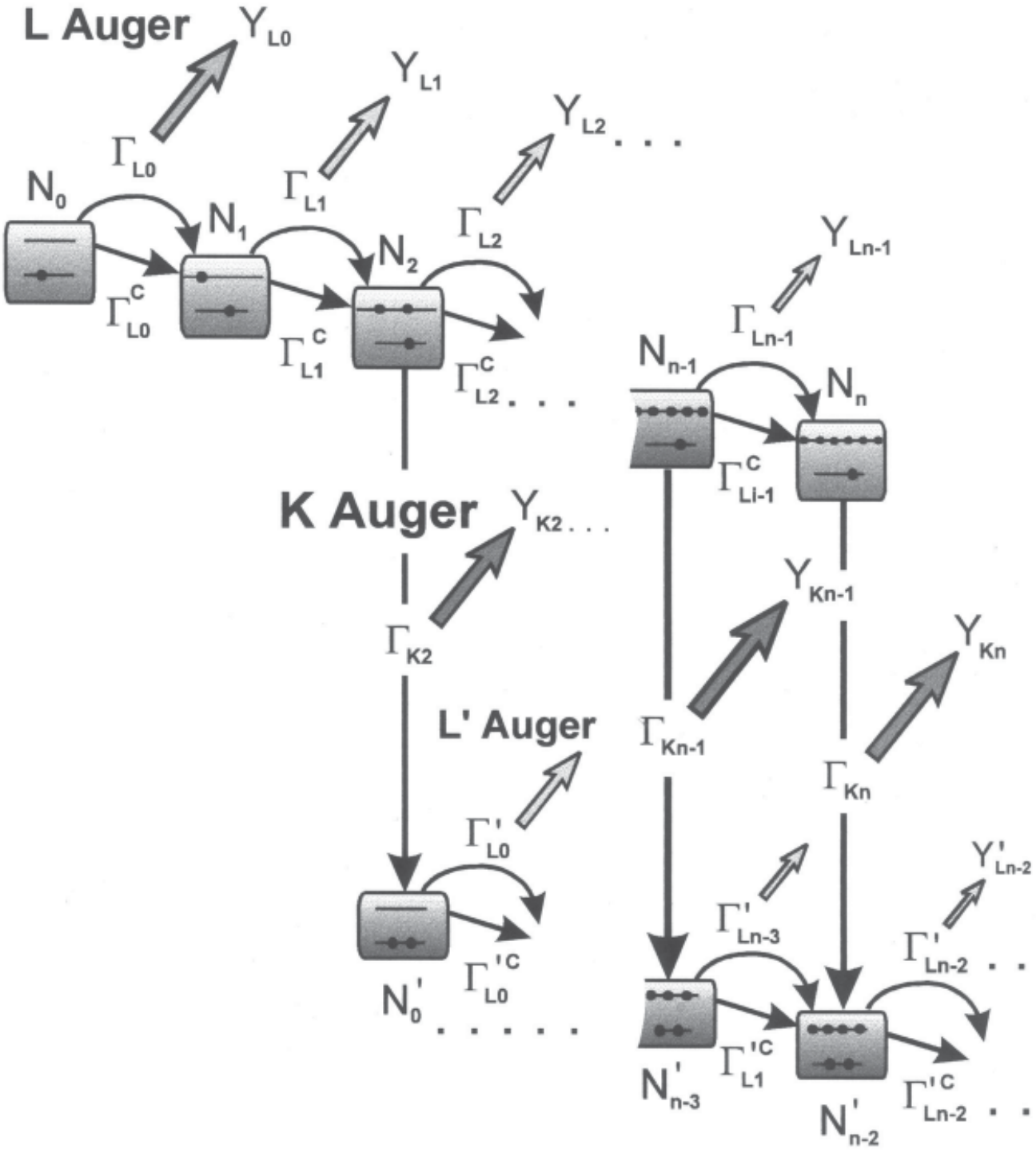


**Figure 6**. Diagram for multiple cascade processes in hollow atoms moving below a surface. The label $n_L$ specifies the number of L-shell electrons. The quantities $\Gamma_{LnL}$ and $\Gamma_{KnL}$ are L- and K-Auger transition rates. The quantities $\Gamma_{nL}$ are rates for collisional transfer of an electron into the L shell. The arrows indicate qualitatively the intensity of the ejected L- and K-Auger electrons.

vacancy and an empty L shell contains 9 electrons in the induced charge cloud. For this case, it is seen that the 1*s* electron density is clearly separated from the induced charge cloud that maximizes near 1.5 a.u. At about 0.8 a.u., the charge density exhibits a deep valley that is a signature of the hollow atom. It is seen from Figure 4 that this signature diminishes as the hollow atom gets more and more filled in the L shell.

To visualize the hollow atom in the solid, Figure 5 shows density plots of the electronic charge cloud. At the bottom of the graph, the corresponding density functions, already given in Figure 4, are plotted. For the first case of an unfilled L shell, the left graph shows a remarkably empty space within the induced electron cloud. It appears that this signature of a hollow atom is magnified in the solid as compared with the vacuum (compare with Fig. 3). As noted before, the hollow atom disappears as the L shell becomes filled. When 6 electrons are located in the L shell, the induced electron density is barely visible.

The filling of the L shell ($n = 2$) is due to charge transfer between inner shells resulting primarily from binary collisions between the projectile and individual target atoms. The details of the processes responsible for the L-shell filling are discussed in the following section.

### Cascade Model for L-shell Filling

The filling sequence of the hollow atom is determined by expressions that are similar to those for the radioactive decay of nuclei known from textbooks [24]. The possible dynamic processes are shown schematically in Figure 6. They depend on various model parameters. For Ne in Al, the filling of the projectile L shell takes place via L-Auger transitions and collisional charge transfer both governed by the L-Auger rate $\Gamma_{LnL}$ and the capture rate $\Gamma_{nL}$, respectively, where $n_L$ is the number of electrons occupying the L shell. The time-dependent number of atoms $N_{nL}(t)$ with one vacancy in the K shell and $n_L$ electrons in the L shell is obtained solving the rate equations [21, 23, 27]:

$$\frac{dN_n}{dt} = \Gamma^f_{Ln-1} N_{n-1} - S_n N_n \qquad (1)$$

where the L-shell filling rate $\Gamma_{nL} = \Gamma_{nL} + \Gamma_{LnL}$ and the sum rate $S_{nL} = \Gamma_{nL} + \Gamma_{KnL}$ are obtained from the individual rates summarized in Table I of Ref. [27]. The rate equation may be solved analytically yielding the number of atoms $N_{nL}(t)$. For $n_L \geq 2$, the ensemble of atoms $N_{nL}(t)$ undergo K-Auger transitions with the rate $\Gamma_{KnL}$. The emission rate of the K-Auger electrons is obtained as $K_{nL}(t) = N_{nL}(t)\,\Gamma_{KnL}$.

Since the Auger electrons are ejected within the solid, the flux of the K-Auger electrons on their way out to the surface is reduced by elastic and inelastic collisions. We assume

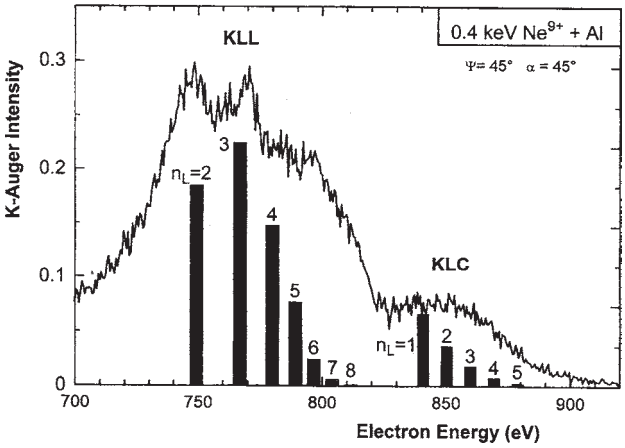


**Figure 7**. Spectrum of K-Auger electrons ejected by interaction of $Ne^{9+}$ ions with an Al surface. The bar diagram is calculated using the cascade model discussed in the text.

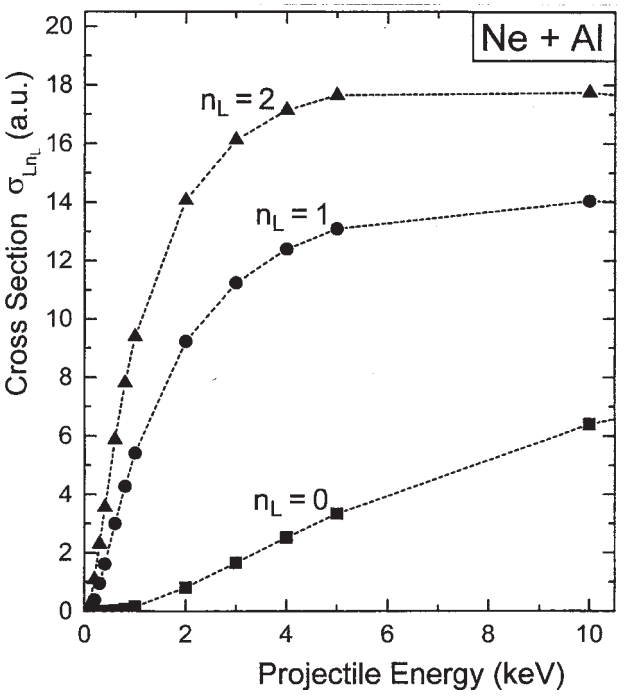


**Figure 8**. Cross sections for charge exchange from Al atoms into hollow neon atoms with the number $Ne^{9+}$ of L shell electrons as a function of the projectile energy. The data are calculated using the Landau-Zener model with potential curves from a previous model by Stolterfoht [25] (see text).

---

an exponential attenuation law $a_K(t) = e^{-\Gamma kt}$, where $\Gamma$ is the attenuation rate. This time-dependent attenuation law follows directly from the well-known expression $a_K(l) = \exp -l/\lambda$ where l is the travel distance of the electrons in the solid, and $\lambda$ is the

corresponding attenuation length. More information is given in Ref. [27].

After time integrating, one obtains the *attenuated intensity* of the Auger electrons in the elastic channel which may be evaluated analytically giving rise to the relatively simple expression [27]:

$$Y^a_{Kn} = \Gamma_{Kn} \frac{\prod_{i=0}^{n-1} \Gamma^f_{Li}}{\prod_{i=0}^{n} \tilde{S}^a_{Ki}} \qquad (2)$$

where 3 is the sum rate modified by attenuation. A similar expression has been given by Limburg *et al*. [18].

The Auger electrons lost by attenuation are primarily scattered into the inelastic channel where the creation of Auger intensity is governed by the *build-up function* $b_K(t) = [1- \exp(\Gamma.t)]. \exp(\Gamma.t)$. Similar as for the primary channel, the flux in the inelastic channel is integrated to obtain the *build-up intensity* $Y_{nL}$ which, in turn, is obtained as the difference of two terms each one analogous to that given in eq. (2).

As the Auger electrons are usually measured within a wide range of energies, covering most of the inelastic energy spectrum, we compare the experiment with the *transported intensity*

$$Y_{KnL} = Y_{nL} + Y_{nL} \qquad (3)$$

The cascade model requires a number of model parameters that have been determined by *a priori* methods in reference [27]. Specifically, the model needs cross sections for charge exchange between molecular inner-shell orbitals correlating with the L shells of the projectile and target atoms.

These molecular orbitals were evaluated using model matrix elements evaluated previously [25]. Then, electron transfer probabilities are determined on the basis of the Landau-Zener model, which, in turn, are used to evaluate the corresponding cross sections that are required in the present model.

### Comparison Between Theory and Experiment

An example for a K-Auger spectrum obtained for $Ne^{9+}$ on Al is given in Figure 7. The dominant peak is due to KLL Auger transitions, and the side peak at higher energies originates from KLC Auger transitions, where C stands for the induced charge cloud (Fig. 1). The spectrum provides information about the filling state of the hollow atom moving in the solid. Auger electrons associated with an increasing number $n_L$ of L-shell electrons are observed at higher energies.

Data from eq. (3) are given as a bar diagram in Figure 7. It is noted that the bar diagram is not shown here with the aim to reproduce exactly the experimental spectrum. Rather, the model results are shown to assist in a qualitative understanding of the spectral structures. As discussed before, the first prominent peak at 748 eV corresponds primarily to Auger transitions from an initial state with a number $n_L = 2$ of 2s electrons. The next peak at higher energies primarily corresponds to $n_L = 3$, but may contain components from $n_L = 2$ where the two electrons are in 2*s* and 2*p* orbitals. The next peak contains Auger intensities due to higher occupation numbers.

In Figure 7, the diagram is composed of bars which maximize at small L-shell occupation numbers. The bars attributed to the numbers $n_L = 2$, 3, and 4 dominate, whereas those due to the higher numbers $n_L = 7$ and 8 are not significant. This is an indication for the K-Auger transitions taking place at the beginning of the L-shell filling sequence. This observation, in turn, is a signature for the fact that the filling of the Ne L shell is relatively slow. The explanation for this finding is that the collisional transfer processes are unimportant at the low projectile energy of 400 eV.

To study the onset of the collisional electron transfer, we performed calculations by means of the Landau-Zener model using model potential curves described in more details previously [25]. The transfer processes occur at curve crossings of potential curves correlating with the L shell orbitals of the collision partner Ne and Al [27]. In Figure 8, the resulting cross sections are shown as a function of the projectile energy for L shell the filling state of $n_L = 0$, 1 and 2. It is seen that the calculated cross sections exhibits indeed a threshold in the projectile energy. This shows that the theoretical cross sections indicate a strong increase of the L-shell filling in a relatively narrow energy range.

To verify the theoretical prediction, we measured K Auger spectra as a function of the projectile energy. Figure 9 shows the results for $Ne^{9+}$ incident at energies from 0.10 to 0.75 keV on Al. A close inspection of the figure indicates that the spectral range around 800 eV attributed to $n_L = 7$ and 8 increases significantly with increasing projectile energy. As a consequence, the structures of the main KLL Auger peaks are increasingly washed out, and the minimum between the KLL and KLC Auger intensity is more and more filled as the projectile energy increases.

This behavior confirms the onset of the colli-sional electron transfer occurring in addition to the L-Auger transitions. It is noted that for a constant capture cross section, the corresponding capture rate that is relevant for the cascade model, is proportional to the projectile velocity [16]. However, the rapid increase of the spectral intensity associated with $n_L$ - 8 in a relatively small energy range suggests that the linear increase of the capture rate is not sufficient to explain the experimental data. Therefore, in accordance with the theoretical results in Figure 8, it is concluded that the electron transfer

cross section varies significantly in the present energy range.

It should be added that the studies of Auger spectra by Limburg *et al.* [17, 18] and X ray spectra by Briand *et al.* [7] are similar to the present one (Fig. 9). In some cases, these authors draw different conclusions for the effects changing the spectral structures. This is partially due to the fact that they used other projectile species and impact energies. For the present cases, it is recalled from the discussion of Figure 3 that outside the solid the emission of K-Auger electron from hollow Ne is very unlikely.

Hence, it follows that the filling of the hollow atom is governed by the charge transfer between inner shells of the projectile and atoms in the solid. From the present model, it is found that at the lowest projectile energies the typical filling time, corresponding to the life time of the hollow atoms, is equal to a few $10^{-14}$ sec. This time is much longer than an interval of a few $10^{-17}$ seconds which corresponds to the time unit for atomic processes.

## Concluding Considerations about Energy Deposition

The preceding discussion has shown that primarily two mechanisms are responsible for the neutralization of a highly charged ion interacting with the surface. First, quasi-resonant charge transfer which involve one active electron, and second, Auger transitions (or Auger-like processes) which involve two active electrons. The latter processes, initiated by electron-electron interaction, are also referred to as **dielectronic processes** [26].

It should be emphasized that these dielectronic processes mediate the transfer of the potential energy of the ion into the solid. To illustrate this type of energy deposition, let us consider a highly charged ion moving in a solid. At small ion energies, i.e., when the kinetic energy of the projectile is significantly lower than its potential energy, the nuclear-electron and nuclear-nuclear interactions considered in textbooks [29] cannot contribute much to the energy deposition into the solid. Other processes have to be considered. As shown in Figure 10, a highly charged ion involves a strong positive charge which attracts electrons so that they are accelerated into the charge center. When neglecting any further interaction, the electron will pass through the ionic center without much effect in view of energy transfer. When the ion is slowly moving, the electron may be captured into highly lying orbitals, but the energy transfer is again small as the capture occurs resonantly. The situation changes considerably as two accelerated electrons hit each other deep inside the ionic center. Hence, a dielectronic process occurs involving an energy loss of one of the electrons so that it cannot escape from the attractive charge. The electron is captured into a lower lying orbital whose binding energy $E_b$ may be significant. Thus, the other electron receives an excess

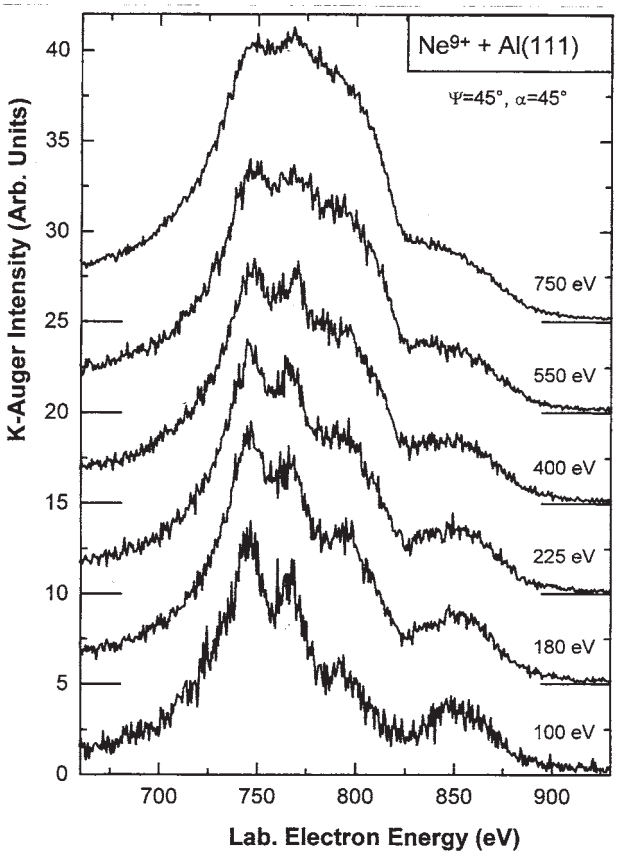


**Figure 9**. Auger spectra produced by $Ne^{9+}$ incident at 45° on an Al surface. The impact energy was varied from 0.1 to 0.75 keV as indicated. The electron observation angle is 45°.

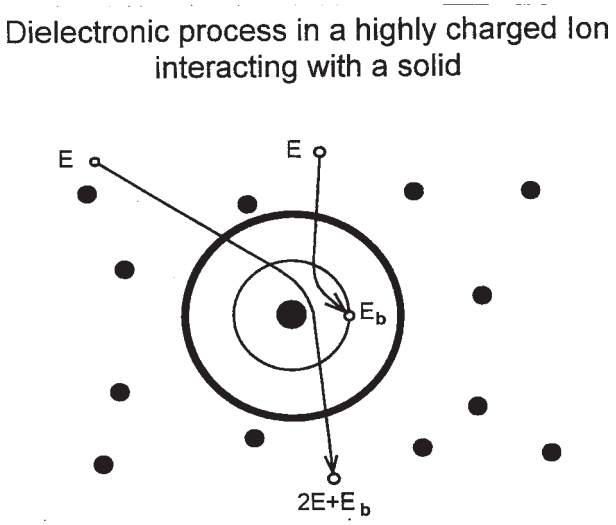


**Figure 10**. Dielectronic process producing energy deposition by highly charged ions moving in a solid with small kinetic energy.

energy equal to $E_b$ (Fig. 10).

The present consideration shows that dielectronic processes are responsible for the exchange of potential energy from the projectile to kinetic energy of the electrons and, hence, they account for the energy deposition by slow, highly charged ions in matter. It should be emphasized that the dielectronic processes are produced by electron-electron interaction, which is generally not considered in energy deposition mechanisms discussed in the literature [29]. Nevertheless, we point out that most of the dielectronic processes are well-known. For instance, in the field of ion atom collisions, the dielectronic process shown in Figure 10 is known as three-body recombination [26]. The dielectronic process which involves an initial bound electron is also referred to as Auger capture [11]. Moreover, the difference between potential and kinetic electron emission has previously been studied in detail [4]. The present discussion does not introduce new processes. Rather, it emphasizes the importance of the dielectronic processes within a family of energy deposition mechanisms well-known from text books.

## Acknowledgments

We are indebted to the groups of Werner Heiland and Jörn Bleck-Neuhaus for long-standing fruitful collaborations. We acknowledge the support by the Human Capital and Mobility program under the contract number CHRT-CT93-0103.

## References

[1] Andrä HJ (1989) Electronic interaction of multicharged ions with metal surfaces at low energies. Nucl. Instr. Methods **B43**: 306-317.

[2] Arifov UA, Mukhamadiev ES, Parilis ES, Pasyuk AS (1973) On the identification of multiply charged ions by electron emission. Sov. Phys. Tech. Phys. **18**: 240-243.

[3] Arnau A, Köhrbrück R, Grether M, Spieler A, Stolterfoht N (1995) Molecular-orbital model for slow hollow atoms colliding with atoms in a solid. Phys. Rev. **A51**: R3399-R3402.

[4] Aumayr F, Winter HP (1994) Emission of slow and fast electrons from clean metal surfaces under impact of slow multicharged ions. Comments At. Mol. Phys. **29**: 275-303.

[5] Aumayr F, Lakits G, Winter HP (1991) On the measurements of statistics for particle-induced electron emission from a clean metal surface. Appl. Surf. Sci. **47**: 139-147.

[6] Borisov AG, Wille U (1996) Resonant electron transfer between highly charged ions and metal surfaces: First-order vs. nonperturbative transition rates. Nucl. Instrum. Meth. Phys. Res. **B115**: 137-141.

[7] Briand JP, de Billy L, Charles P, Essabaa S, Briand P, Geller R, Desclaux JP, Bliman S, Ristori C (1990) Production of hollow atoms by the excitation of highly charged ions in interaction with a metallic surface. Phys. Rev. Lett. **65**: 159-162.

[8] Burgdörfer J (1993) Atomic collisions with surfaces. In: Review of Fundamental Processes and Applications of Atoms and Ions. Lin CD (ed.). World Scientific, Singapore. p. 517.

[9] Burgdörfer J, Lerner P, Meyer FW (1991) Above-surface neutralization of highly charged ions: The classical over-the-barrier model. Phys. Rev. **A44**: 5674-5685.

[10] Cowan RD (1981) The Theory of Atomic Structure and Spectra. University of California Press, Berkeley. pp. 10-31.

[11] Echenique PM, Flores F, Ritchie RH (1990) Dynamic screening of ions in matter. In: Solid State Physics: Advances in Research and Applications. Vol. 43. Ehrenreich H, Turnbull D (eds.). Academic Press, New York. pp. 230-306.

[12] Folkerts L, Morgenstern R (1990) Auger electrons resulting from slow H-like ions neutralized near a Tungsten surface. Europhys. Lett. **13**: 377.

[13] Grether M, Spieler A, Köhrbrück R, Stolterfoht N (1995) Dynamic *K*- and *L*- shell filling of $Ne^{9+}$ projectiles interacting with an Al(111) surface. Phys. Rev. **A524**: 26-31.

[14] Itoh A, Schneider D, Schneider T, Zouros TJ, Nolte G, Schiwietz G, Zeitz W, Stolterfoht N (1985) Selective production of Li-, Be-, and B-Like K-vacancy states in fast Ne projectiles studied by zero-degree Auger spectroscopy. Phys. Rev. **A31**: 684-92.

[15] Köhrbrück R, Sommer K, Biersack JP, Bleck-Neuhaus J, Schippers S, Roncin P, Lecler D, Fremont F, Stolterfoht N (1992) Auger-electron emission from slow highly charged ions interacting with solid Cu targets. Phys. Rev. **A45**: 4653-4660.

[16] Köhrbrück R, Grether M, Spieler A, Stolterfoht N, Page R, Saal A, Bleck-Neuhaus J (1994) Angular distribution of K Auger electrons ejected by highly charged ions interacting with an Al(111) surface. Phys. Rev. **A50**: 1429-1434.

[17] Limburg H, Das J, Schippers S, Hoekstra R, Morgenstern R (1994) The interaction of hydrogenic ion with metal and semiconductor surfaces. Surf. Sci. **313**: 355-364.

[18] Limburg H, Schippers S, Hughes I, Hoekstra R, Morgenstern R, Hustedt S, Hatke N, Heiland W (1995) Velocity dependence of KLL Auger emission from hollow atoms formed during collisions of hydrogenic $N^{6+}$ ions on surfaces. Phys. Rev. **A51**: 3873-3882.

[19] Martin B, Grether M, Köhrbrück R, Stettner U, Waldmann H (1993) The Berlin 14.5 GHz ECR ion source and its testbench for the production of slow highly charged ions. In: Proceedings of the 11th International Workshop on Electron Cyclotron Resonance Ion. University Press, Groningen, The Netherlands. pp. 188-189.

[20] Meyer FW, Overbury SH, Havener CC, Zeijlmans

van Emmichoven PA, Zehner DM (1991) Evidence for above-surface and subsurface neutralization during interactions of highly charged ions with a metal target. Phys. Rev. Lett. **67**: 723-726.

[21] Page R, Saal A, Thomaschewski J, Aberle L, Bleck-Neuhaus J, Köhrbrück R, Grether M, Spieler A, Stolterfoht N (1995) Multistep cascade model for the de-excitation of highly charged ions impinging on a solid surface. Phys. Rev. **A52**: 1344-1353.

[22] Schippers S, Hustedt S, Heiland W, Köhrbrück R, Kemmler J, Lecler F, Bleck-Neuhaus J, Stolterfoht N (1992) Excitation of target Auger-electron emission by the impact of highly charged ions: $N^{6+}$, $O^{7+}$, and $Ne^{9+}$ on Pt(110). Phys. Rev. **A46**: 4003-4011.

[23] Schippers S, Limburg J, Das J, Hoekstra R, Morgenstern R (1994) Atomic structure calculations of KLL Auger spectra from highly charged ion-solid-surface collisions. Phys. Rev. **A50**: 540-552.

[24] Segré E (1964) Nuclei and Particles. WA Benjamin Inc., New York. pp. 256-277.

[25] Stolterfoht N (1987) Near resonant vacancy exchange between inner shells of colliding heavy particles. In: Progress in Atomic Spectroscopy. Part D. Kleinoppen H (ed.). Plenum Press, New York. pp. 415-476.

[26] Stolterfoht N (1991) Dielectronic processes and electron correlation in energetic ion-atom collisions. Nucl. Instr. Meth. **B53**: 477-492.

[27] Stolterfoht N, Arnau A, Grether M, Köhrbrück R, Spieler A, Page R, Saal A, Thomaschewski J, Bleck-Neuhaus J (1995) Multiple-cascade model for the filling of hollow atoms moving below an Al surface. Phys. Rev. **A52**: 445-456.

[28] Zaremba E, Sander LM, Shore HB, Rose JH, (1977) Self-consistent screening of a proton in jellium. J. Phys. **F7**: 1763-1772.

[29] Ziegler JI, Biersack JP, Littmark U (1985) The Stopping and Ranges of Ions in Matter. Vol. I. Pergamon Press, New York. pp. 21-76.

**Editor's Note**: All of the reviewers' concerns were appropriately addressed by text changes, hence there is no **Discussion with Reviewers**.